

Electronic Relaxation Pathways of Thio-Acridone and Thio-Coumarin: Two Heavy-Atom-Free Photosensitizers Absorbing Visible Light

Chris Acquah,¹ Sean Hoehn,¹ Sarah Krul,¹ Steffen Jockusch,² Shudan Yang,³ Sourav Kanti Seth,¹ Eric Lee,¹ Han Xiao,^{3,4,5,6} & Carlos E. Crespo-Hernández,^{*1}

¹ Department of Chemistry, Case Western Reserve University, Cleveland, OH 44106, USA

² Center for Photochemical Sciences, Bowling Green State University, Bowling Green, Ohio, 43403, USA

³ Department of Chemistry, Rice University, 6100 Main Street, Houston, Texas, 77005, USA

⁴ Department of Biosciences, Rice University, 6100 Main Street, Houston, Texas, 77005, USA

⁵ Department of Bioengineering, Rice University, 6100 Main Street, Houston, Texas, 77005, USA

⁶ SynthX Center, Rice University, 6100 Main Street, Houston, Texas, 77005, USA

*Corresponding author; E-mail: carlos.crespo@case.edu, ORCID: 000-0002-3594-0890.

Supporting Information

S1. Methods	2
S1.1. Materials and steady-state measurements.....	2
S1.2. Quantum chemical calculations.....	2
S1.3. Broadband femtosecond transient absorption spectroscopy.....	2
S1.4. Laser flash photolysis.....	3
S1.5. Singlet oxygen quantum yields.....	3
S2. Supporting experimental and computational results	5
S2.1. Simulated steady-state absorption.....	5
S2.2. Steady-state emission and excitation.....	6
S2.3. Theoretical results.....	9
S2.4. Calculated excited state absorption spectra.....	22
S3. Cartesian coordinates of relevant states	24
S4. Supporting references	32

S1. Methods

S1.1 Materials and steady-state measurements

Thio-acridone (SACD) and thio-coumarin (SCou) were obtained and prepared as described by Xiao et al.¹ The synthesis procedure and characterization of the molecules including ¹H NMR, ESI-MS, FT-IR, etc. can be found in the cited literature.¹ Solutions of both compounds were prepared in HPLC and spectrophotometric grade Acetonitrile (ACN) and Dimethyl Sulfoxide (DMSO) from Sigma-Aldrich and maintained under dark conditions to prevent degradation. Polar aprotic solvents such as ACN and DMSO were chosen due to the compounds' higher solubility compared to polar protic solvents like water. Additionally, the absence of coherent signals in ACN during transient experiments made it an ideal choice. Steady-state absorption and emission spectra were recorded using a Jasco V-130 Spectrophotometer and Cary Eclipse spectrometer, respectively. Excitation and emission spectra were obtained using a PMT voltage of 600V with 5 nm slit widths and a scan rate of 120 nm/min. Solutions for emission and excitation spectra were prepared with an optical density of ~0.08 at the excitation wavelength of 470 nm.

S1.2 Quantum chemical calculations

The ORCA 5.0.2 software package was used to perform density functional theory (DFT) and time-dependent DFT (TD-DFT) calculations.² Ground-state optimizations were performed using the B3LYP/G functionals and the def2-TZVPD basis set.^{3,4} Bulk implicit solvation effects will be modeled using the conductor-like polarizable continuum model (CPCM).⁵ VEEs were calculated at the TD-PBE0-D3BJ/CPCM/def2-TZVPD level of theory. The choice of functional for the VEE and SOCs was made based on the HAF-PSs at study. However, based on our experience with other HAF-PSs and their satisfactory performance, the PBE0, CAM-B3LYP, and X3LYP were tested first. The def2-TZVPD basis set and the CPCM were used in the TD-DFT calculations as well.

S1.3 Broadband femtosecond transient absorption spectroscopy

The transient absorption setup used has been described in detail in previous publications.^{6,7} Briefly, the TAS spectrometer (Helios, Ultrafast Systems) uses a Ti:Sapphire oscillator (Vitesse, Coherent) that seeds a regenerative amplifier (Libra-HE, Coherent), generating pulses of 100 fs (1 kHz and

800 nm). The excitation wavelength was generated by using an optical parametric amplifier (TOPAS, Quantronix/Light Conversion). A translating 2 mm CaF₂ crystal generates the white light continuum, which gives access to a spectral range from 320 to 700 nm to probe the excited state dynamics.

During the TAS experiments, the absorbance of the samples at the excitation wavelength was 0.5 and OD matched for all runs. The sample was also continually stirred with a Teflon-coated magnetic stir bar to maintain the homogeneity of the solutions. Additionally, samples were frequently refreshed with fresh samples after each scan to minimize contamination of transient signals. A home-made LabView program and Surface Explorer software (Ultrafast Systems) were used for the data collection while the Glotaran graphical user interface with R-package TIMP software⁸ was used for the target data and global analyses. Three and four sequential kinetic models were used to globally fit the full multidimensional data set for SACD and SCou. Finally, the evolution-associated difference spectra (EADS) were extracted from the global and target analysis.⁸

S1.4 Nanosecond laser flash photolysis

Nanosecond laser flash photolysis experiments were used to characterize the triplet state of SACD and SCou. These experiments employed pulses generated by a Brilliant Nd:YAG laser (Quantel) in conjunction with a Vibrant OPO (OPOTEC) for excitation at 470 nm (5 ns pulse width) and a computer-controlled system that has been described in detail elsewhere.⁹ Experiments were performed in a 1 cm optical cell with an absorbance at the excitation wavelength of ~0.3 in acetonitrile. Deoxygenated solutions were prepared by purging with argon gas for at least 20 min.

S1.5 Singlet oxygen quantum yields

Time-resolved luminescence spectroscopy was used to determine the singlet oxygen quantum yields for SACD and SCou. A Brilliant Nd:YAG laser (Quantel) in conjunction with a Vibrant OPO (OPOTEC) (420 nm, 5 ns pulse width) was used as the excitation source for both molecules. Singlet oxygen phosphorescent decay traces were collected at 1270 nm using a modified

Fluorolog-3 spectrometer (HORIBA, Jobin Yvon), with a near-IR sensitive photomultiplier tube (H10330A-45, Hamamatsu) as a detector. The decay traces were stored on a digital oscilloscope (TDS 360, Tektronics). Solutions of SACD, SCou, and the phenalenone standard were prepared in acetonitrile at an optical density of 0.3 at the excitation wavelength in 1 cm path-length quartz cuvettes. Degradation of the samples was determined to be less than 3% throughout the experiments based on their steady-state absorption spectra.

The quantum yields were determined in back-to-back luminescence experiments of SACD, SCou, and Phenalenone solutions under the same conditions, using the reported yield of $^1\text{O}_2$ generated by phenalenone as a standard ($\Phi_{\Delta} = 0.98$).¹⁰

S2. Supporting experimental and computational results and discussion

S2.1 Simulated steady-state absorption

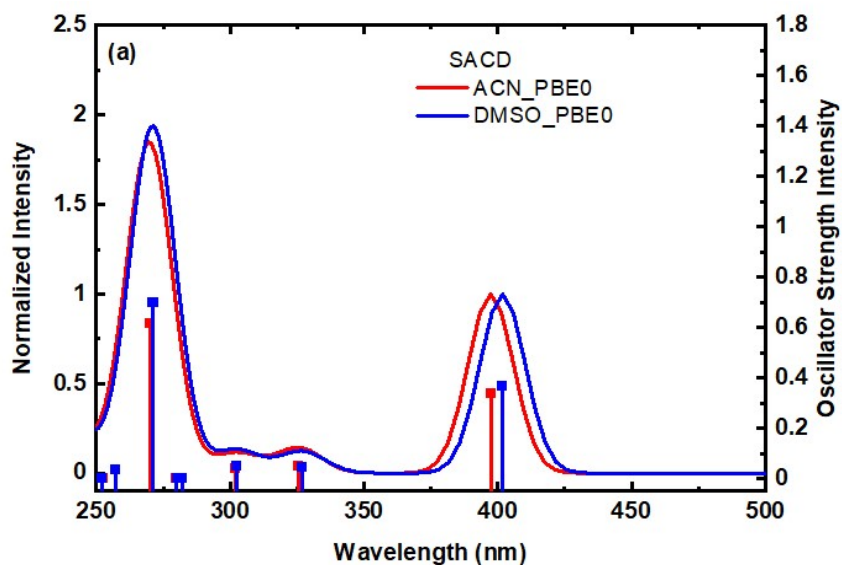
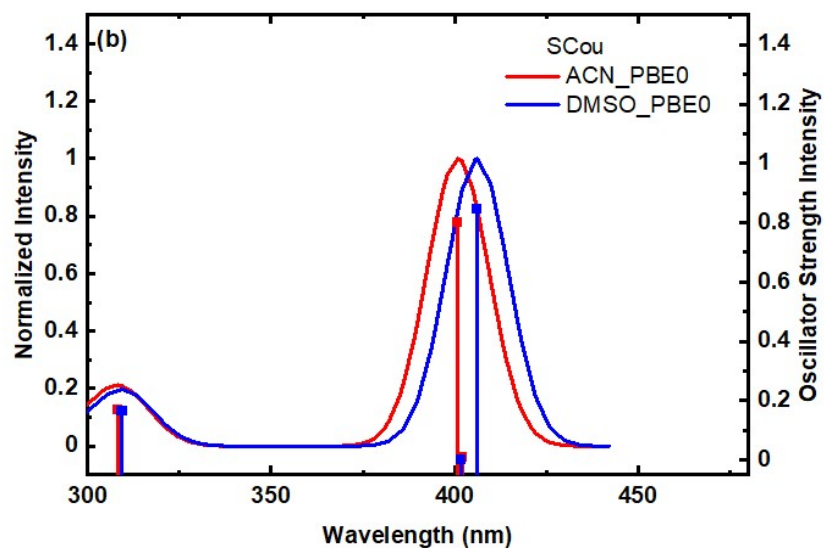


Figure S1. Normalized simulated absorption spectra of a) SAcD and b) SCou in ACN and DMSO computed at the TD-PBE0-D3BJ/CPCM/def2-TZVPD//B3LYP_C-D3BJ/CPCM/def2-TZVPD level of theory.

S2.2 Steady state emission and excitation



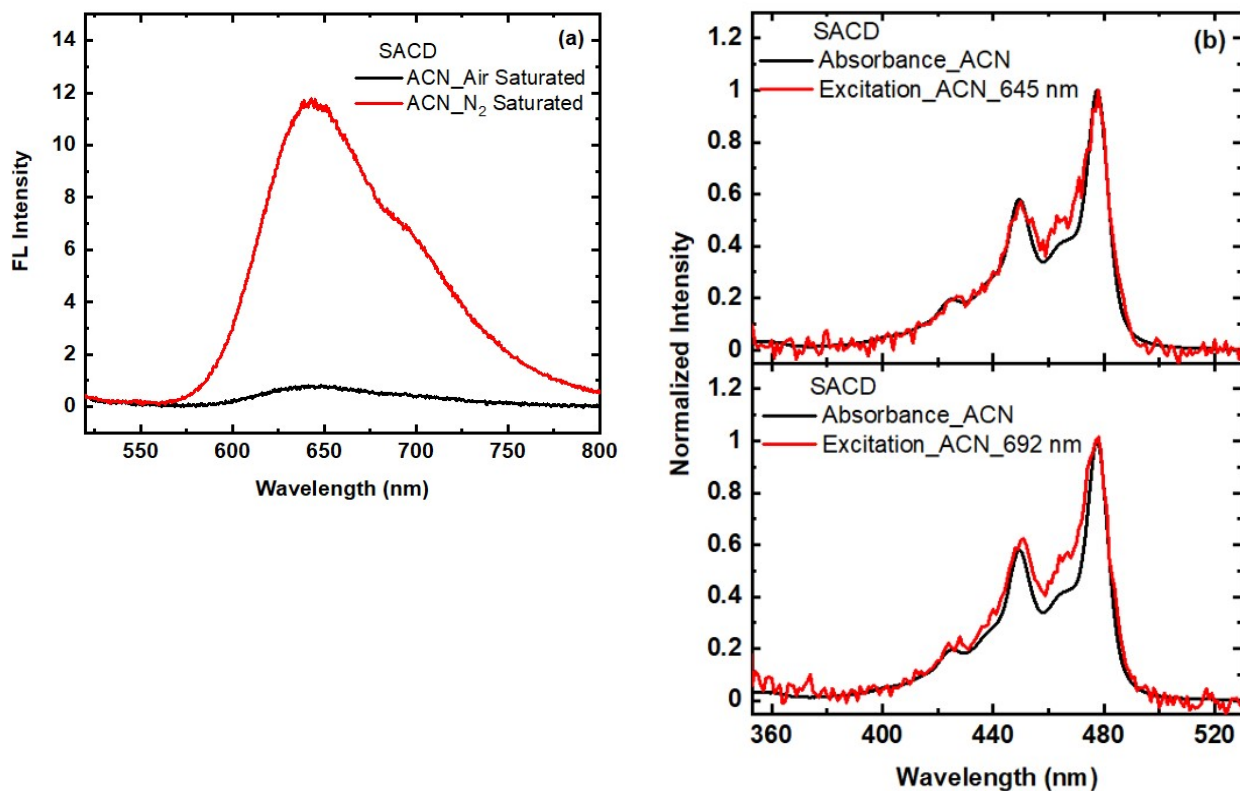


Figure S2. a) Emission spectra of SCD in ACN under air and N₂ saturated conditions. b) Normalized steady-state excitation and absorption spectra of SCD in ACN following emission at their respective maxima of 645 nm and 692 nm. Excitation spectra were collected using a PMT voltage of 600 V, 5 nm slit widths, and a scan rate of 120 nm/min.

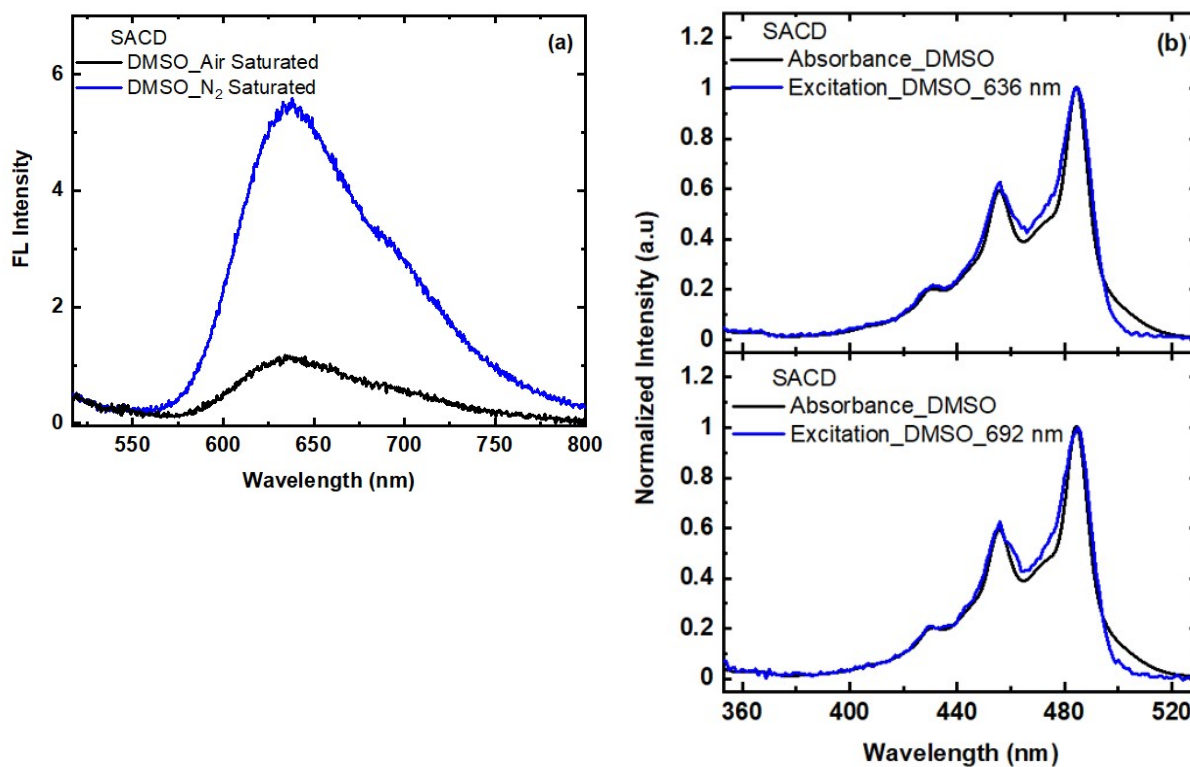


Figure S3. a) Emission spectra of SACD in DMSO under air and N₂ saturated conditions. b) Normalized steady-state excitation and absorption spectra of SACD in DMSO following emission at their respective maxima of 636 nm, and 692 nm. Excitation spectra were collected using a PMT voltage of 600 V, 5 nm slit widths, and a scan rate of 120 nm/min.

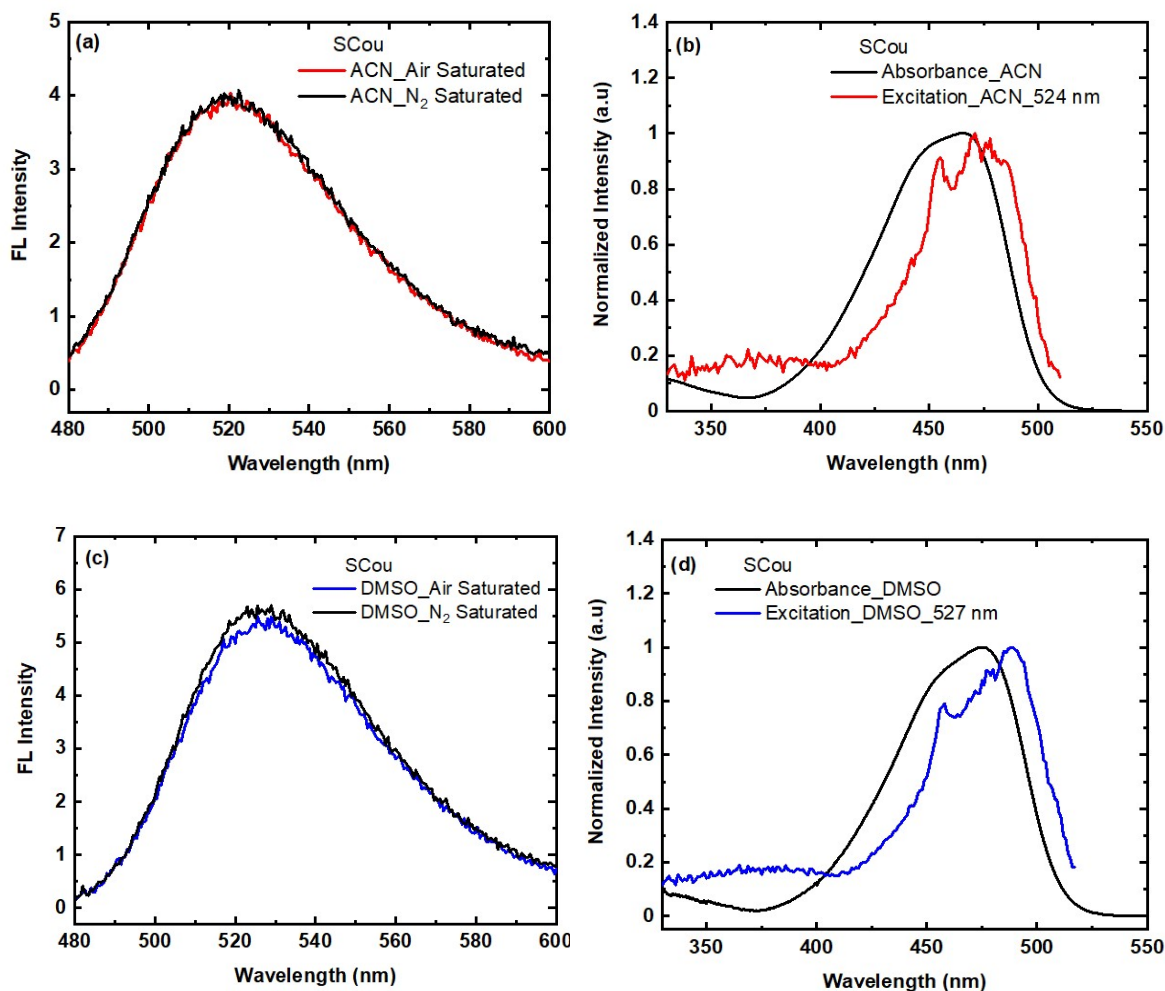


Figure S4. a) Emission spectra of SCou in (a) ACN and (c) DMSO under air and N₂ saturated conditions. Normalized steady-state excitation and absorption spectra of SCou in (b) ACN and (d) DMSO following emission at their respective maxima of 523 nm and 527 nm. Excitation spectra were collected using a PMT voltage of 600 V, 5 nm slit widths, and a scan rate of 120 nm/min.

Table S1. Functional analysis for calculation of vertical excitation energies for the lowest lying singlet and triplet states in the Franck-Condon region for SADC in ACN with the def2-TZVPD basis set.

State	CAM-B3LYP	State	X3LYP	State	PBE0	PBE0 (TDA OFF)
S ₁ (nπ*)	2.62 (0.000)	S ₁ (nπ*)	2.32 (0.000)	S ₁ (nπ*)	2.39 (0.000)	2.37 (0.000)
S ₂ (ππ*)	3.24 (0.417)	S ₂ (ππ*)	3.07 (0.331)	S ₂ (ππ*)	3.12 (0.338)	2.93 (0.241)
S ₃ (ππ*)	4.12 (0.017)	S ₃ (ππ*)	3.71 (0.046)	S ₃ (ππ*)	3.81 (0.047)	3.69 (0.027)
T ₁ (ππ*)	2.08	T ₁ (ππ*)	1.99	T ₁ (ππ*)	1.99	1.87
T ₂ (nπ*)	2.39	T ₂ (nπ*)	2.11	T ₂ (nπ*)	2.15	2.12
T ₃ (ππ*)	3.04	T ₃ (ππ*)	2.83	T ₃ (ππ*)	2.84	2.64
T ₄ (ππ*)	3.55	T ₄ (ππ*)	3.43	T ₄ (ππ*)	3.44	3.18

Table S2. Functional analysis for calculation of vertical excitation energies for the lowest lying singlet and triplet states in the Franck-Condon region for SADC in DMSO with the def2-TZVPD basis set.

State	CAM-B3LYP	State	X3LYP	State	PBE0	PBE0 (TDA OFF)
S ₁ (nπ*)	2.62 (0.000)	S ₁ (nπ*)	2.32 (0.000)	S ₁ (nπ*)	2.39 (0.000)	2.38 (0.000)
S ₂ (ππ*)	3.20 (0.442)	S ₂ (ππ*)	3.03 (0.356)	S ₂ (ππ*)	3.09 (0.365)	2.91 (0.265)
S ₃ (ππ*)	4.11 (0.015)	S ₃ (ππ*)	3.70 (0.043)	S ₃ (ππ*)	3.79 (0.045)	3.68 (0.027)
T ₁ (ππ*)	2.08	T ₁ (ππ*)	1.99	T ₁ (ππ*)	1.99	1.88
T ₂ (nπ*)	2.39	T ₂ (nπ*)	2.11	T ₂ (nπ*)	2.15	2.12
T ₃ (ππ*)	3.04	T ₃ (ππ*)	2.83	T ₃ (ππ*)	2.84	2.64
T ₄ (ππ*)	3.55	T ₄ (ππ*)	3.43	T ₄ (ππ*)	3.44	3.18

Table S3. Functional analysis for calculation of vertical excitation energies for the lowest lying singlet and triplet states in the Franck-Condon region for SCou in ACN with the def2-TZVPD basis set.

State	CAM-B3LYP	State	X3LYP	State	PBE0	PBE0 (TDA OFF)
S ₁ (ππ*)	3.25 (0.928)	S ₁ (nπ*)	3.01 (0.000)	S ₁ (nπ/ππ*)	3.08 (0.007)	2.38 (0.000)
S ₂ (nπ*)	3.33 (0.000)	S ₂ (ππ*)	3.03 (0.780)	S ₂ (ππ/nπ*)	3.09 (0.802)	2.91 (0.265)
S ₃ (ππ*)	4.38 (0.074)	S ₃ (ππ*)	3.93 (0.184)	S ₃ (ππ*)	4.09 (0.171)	3.68 (0.027)
T ₁ (ππ*)	2.17	T ₁ (ππ*)	2.05	T ₁ (ππ*)	2.06	1.88
T ₂ (nπ*)	3.09	T ₂ (nπ*)	2.79	T ₂ (nπ*)	2.84	2.12
T ₃ (ππ*)	3.22	T ₃ (ππ*)	2.99	T ₃ (ππ*)	3.02	2.64
T ₄ (ππ*)	3.83	T ₄ (ππ*)	3.56	T ₄ (ππ*)	3.59	3.18

Table S4. Functional analysis for calculation of vertical excitation energies for the lowest lying singlet and triplet states in the Franck-Condon region for SCoU in DMSO with the def2-TZVPD basis set.

State	CAM-B3LYP	State	X3LYP	State	PBE0	PBE0 (TDA OFF)
S ₁ ($\pi\pi^*$)	3.20 (0.954)	S ₁ ($\pi\pi^*$)	2.99 (0.814)	S ₁ ($\pi\pi^*$)	3.05 (0.845)	2.89 (0.673)
S ₂ ($n\pi^*$)	3.33 (0.000)	S ₂ ($n\pi^*$)	3.01 (0.003)	S ₂ ($n\pi^*$)	3.09 (0.000)	3.08 (0.000)
S ₃ ($\pi\pi^*$)	4.36 (0.079)	S ₃ ($\pi\pi^*$)	3.92 (0.179)	S ₃ ($\pi\pi^*$)	4.01 (0.166)	3.89 (0.102)
T ₁ ($\pi\pi^*$)	2.17	T ₁ ($\pi\pi^*$)	2.05	T ₁ ($\pi\pi^*$)	2.06	1.96
T ₂ ($n\pi^*$)	3.10	T ₂ ($n\pi^*$)	2.79	T ₂ ($n\pi^*$)	2.85	2.82
T ₃ ($\pi\pi^*$)	3.22	T ₃ ($\pi\pi^*$)	2.99	T ₃ ($\pi\pi^*$)	3.02	2.92
T ₄ ($\pi\pi^*$)	3.83	T ₄ ($\pi\pi^*$)	3.56	T ₄ ($\pi\pi^*$)	3.59	3.39

Table S5. Vertical energies and percent contributions for the relevant singlet and triplet transitions of SAcD in ACN calculated at the TD-PBE0-D3BJ/CPCM/def2-TZVPD//B3LYP_G-D3BJ/CPCM/def2-TZVPD level of theory. Primary character of the transition showed in parentheses.

State	Transition	% Contribution	Energy
S ₁ ($n\pi^*$)	H-1 → L+0	98.8	2.34 eV
S ₂ ($\pi\pi^*$)	H-0 → L+0	97.6	2.93 eV
S ₃ ($\pi\pi^*$)	H-2 → L+0	98.4	3.67 eV
T ₁ ($\pi\pi^*$)	H-0 → L+0	96.6	1.87 eV
T ₂ ($n\pi^*$)	H-1 → L+0	97.8	2.12 eV
T ₃ ($\pi\pi^*$)	H-2 → L+0	86.9	2.64 eV
T ₄ ($\pi\pi^*$)	H-3 → L+0	35.4	3.18 eV
	H-4 → L+0	22.2	
	H-0 → L+1	16.2	

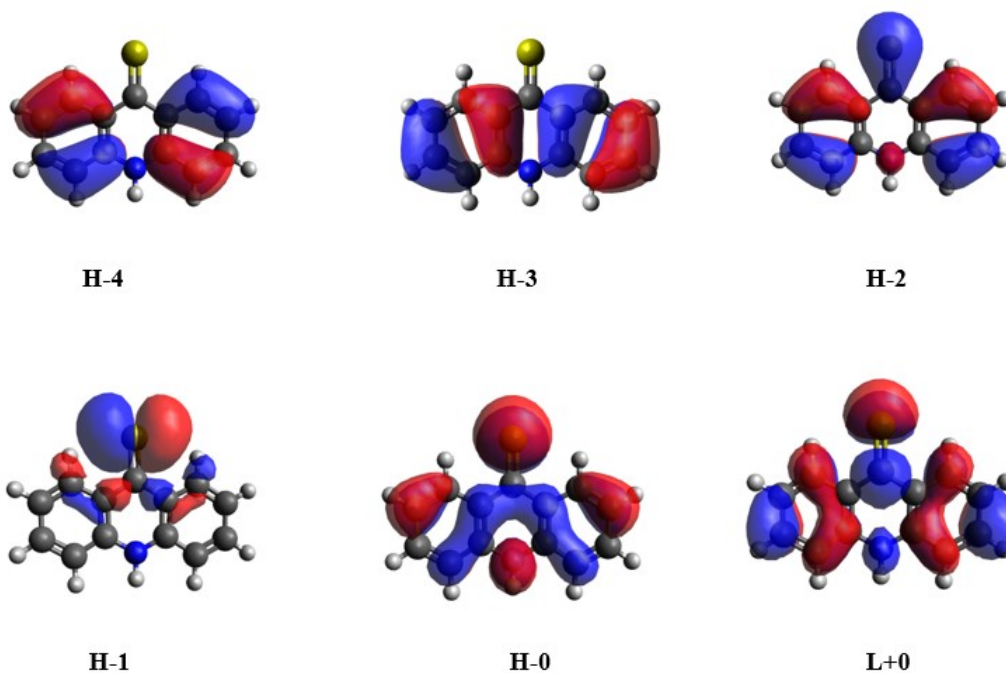


Figure S5. Kohn-Sham orbitals that contribute to the relevant singlet and triplet vertical transitions of SACD in ACN calculated at the TD-CAM-B3LYP-D3BJ/CPCM/def2-TZVPD//B3LYP_G-D3BJ/CPCM/def2-TZVPD level of theory.

Table S6. Vertical energies and percent contributions for the relevant singlet and triplet transitions of SACD in DMSO calculated at the TD-PBE0-D3BJ/CPCM/def2-TZVPD//B3LYP_G-D3BJ/CPCM/def2-TZVPD level of theory. Primary character of the transition showed in parentheses.

State	Transition	% Contribution	Energy
S ₁ (nπ [*])	H-1 → L+0	98.8	2.37 eV
S ₂ (ππ [*])	H-0 → L+0	97.9	2.91 eV
S ₃ (ππ [*])	H-2 → L+0	98.6	3.68 eV
T ₁ (ππ [*])	H-0 → L+0	96.6	1.88 eV
T ₂ (nπ [*])	H-1 → L+0	97.8	2.12 eV
T ₃ (ππ [*])	H-2 → L+0	87.0	2.64 eV
T ₄ (ππ [*])	H-3 → L+0	35.4	3.18 eV

	H-4 \rightarrow L+0	22.3	
	H-0 \rightarrow L+1	15.9	

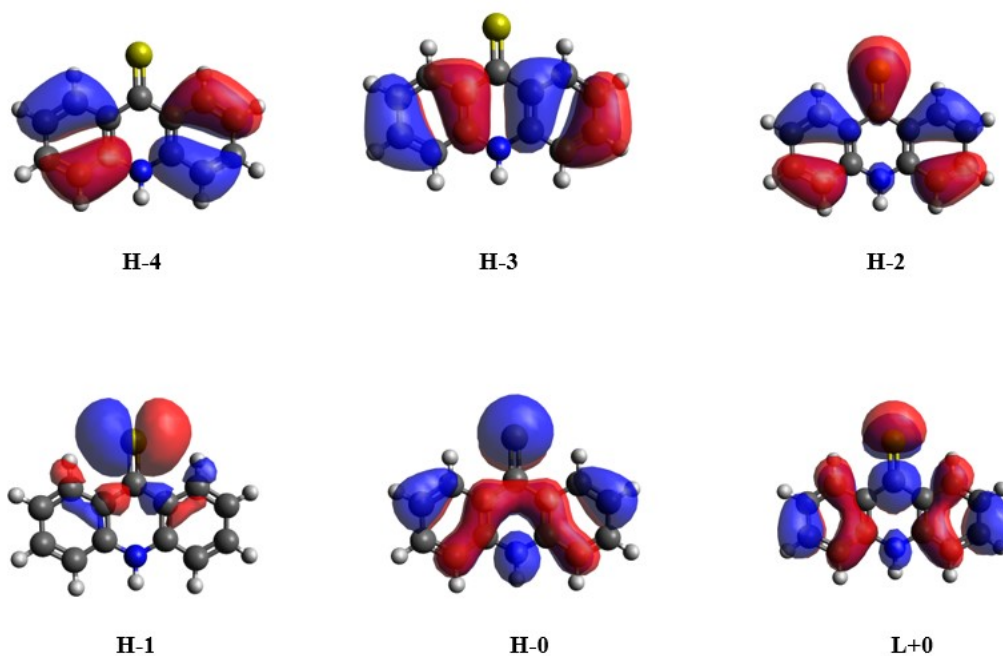


Figure S6. Kohn-Sham orbitals that contribute to the relevant singlet and triplet vertical transitions of SACD in DMSO calculated at the TD-CAM-B3LYP-D3BJ/CPCM/def2-TZVPD//B3LYP_G-D3BJ/CPCM/def2-TZVPD level of theory.

Table S7. Vertical energies and percent contributions for the relevant singlet and triplet transitions of SCou in ACN calculated at the TD-PBE0-D3BJ/CPCM/def2-TZVPD//B3LYP_G-D3BJ/CPCM/def2-TZVPD level of theory. Primary character of the transition showed in parentheses.

State	Transition	% Contribution	Energy
S₁($\pi\pi^*$)	H-0 \rightarrow L+0	97.9	2.93 eV
S₂($n\pi^*$)	H-1 \rightarrow L+0	97.2	3.07 eV
S₃($\pi\pi^*$)	H-2 \rightarrow L+0	92.7	3.90 eV
T₁($\pi\pi^*$)	H-0 \rightarrow L+0	92.6	1.96 eV
T₂($n\pi^*$)	H-1 \rightarrow L+0	95.5	2.81 eV
T₃($\pi\pi^*$)	H-2 \rightarrow L+0	78.8	2.92 eV

$T_4(\pi\pi^*)$	H-0 \rightarrow L+0	51.9	3.39 eV
	H-3 \rightarrow L+1	29.3	

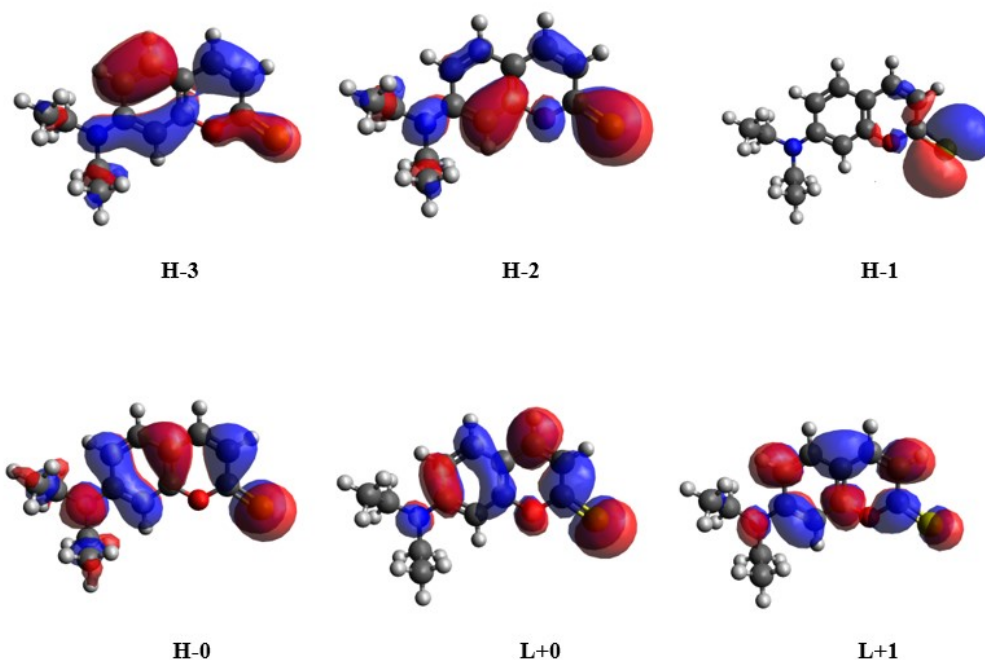


Figure S7. Kohn-Sham orbitals that contribute to the relevant singlet and triplet vertical transitions of SCou in ACN calculated at the TD-CAM-B3LYP-D3BJ/CPCM/def2-TZVPD//B3LYP_G-D3BJ/CPCM/def2-TZVPD level of theory.

Table S8. Vertical energies and percent contributions for the relevant singlet and triplet transitions of SCou in DMSO calculated at the TD-PBE0-D3BJ/CPCM/def2-TZVPD//B3LYP_G-D3BJ/CPCM/def2-TZVPD level of theory. Primary character of the transition showed in parentheses.

State	Transition	% Contribution	Energy
$S_1(\pi\pi^*)$	H-0 \rightarrow L+0	98.1	2.89 eV
$S_2(n\pi^*)$	H-1 \rightarrow L+0	97.2	3.08 eV
$S_3(\pi\pi^*)$	H-2 \rightarrow L+0	93.2	3.89 eV
$T_1(\pi\pi^*)$	H-0 \rightarrow L+0	92.7	1.96 eV
$T_2(n\pi^*)$	H-1 \rightarrow L+0	95.4	2.82 eV
$T_3(\pi\pi^*)$	H-2 \rightarrow L+0	79.0	2.92 eV

$T_4(\pi\pi^*)$	H-0 \rightarrow L+0	51.7	3.39 eV
	H-3 \rightarrow L+1	29.6	

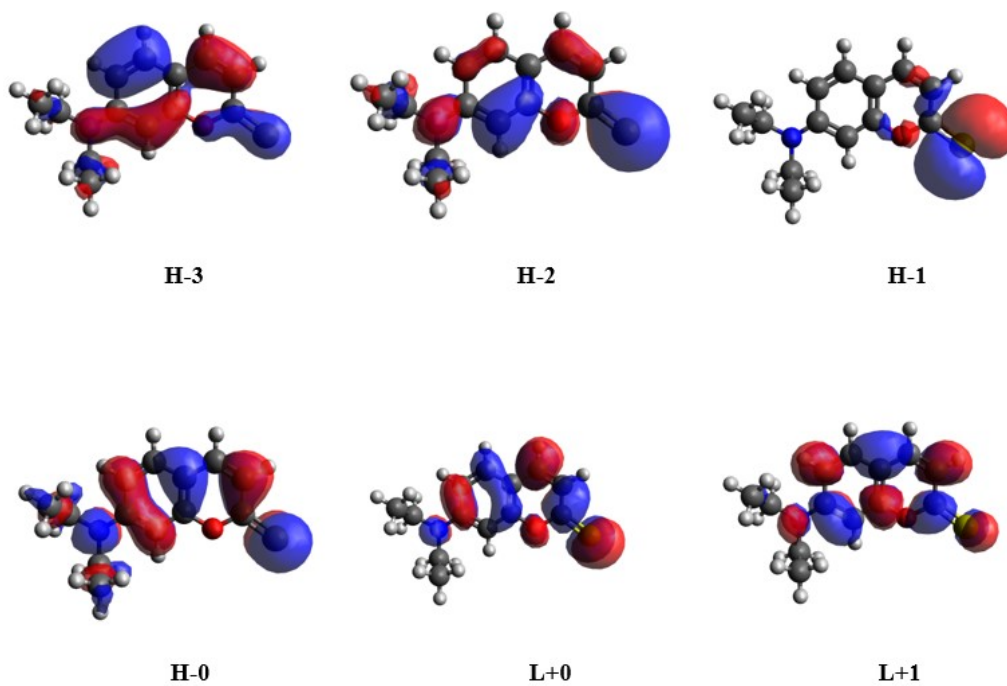


Figure S8. Kohn-Sham orbitals that contribute to the relevant singlet and triplet vertical transitions of SCou in DMSO calculated at the TD-CAM-B3LYP-D3BJ/CPCM/def2-TZVPD//B3LYP_G-D3BJ/CPCM/def2-TZVPD level of theory.

To ascertain the planarity of the optimized geometries, the torsional angles of the primary chromophore in both molecules were adjusted out of the plane by approximately ± 60 degrees. Subsequently, re-optimization was conducted using the same TD-PBE0/CPCM/def2-TZVPD level of theory in both solvents. Figure S9 and S10 displays the re-optimized geometries of the pertinent excited states of SACD and SCou respectively. Evidently, the minimum energy structures of S_1 , S_2 , and T_1 reverted to a planar configuration in both molecules.

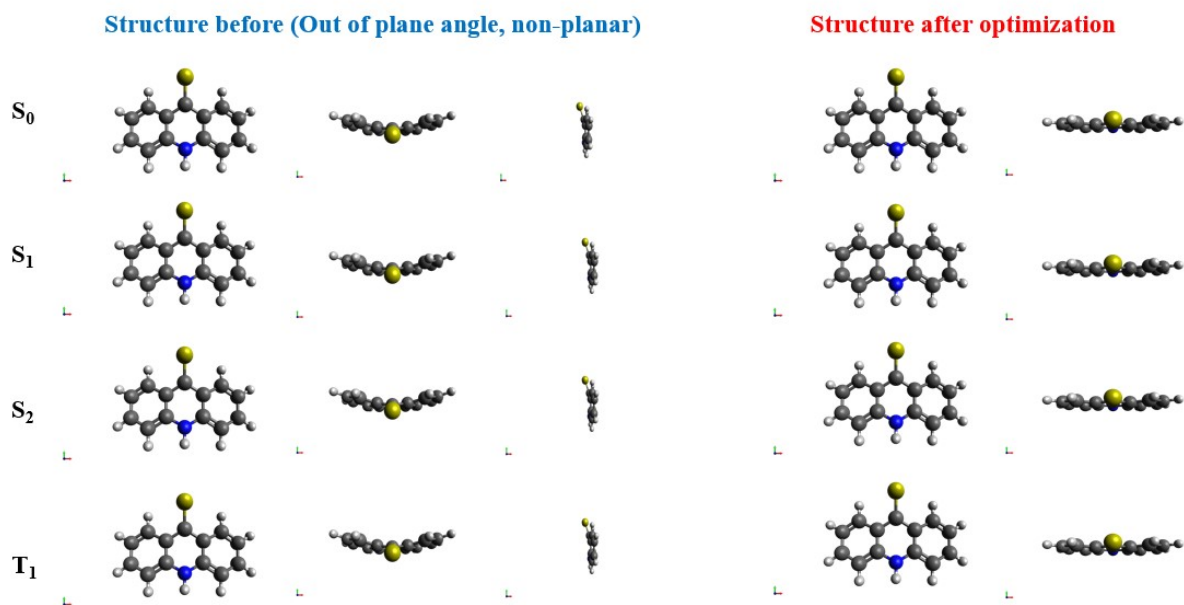


Figure S9. Re-optimized excited geometries of relevant excited states for SACD at the TD PBE0/CPCM/def2-TZVPD level of theory using the purposely induced non-planar structure as a starting point.

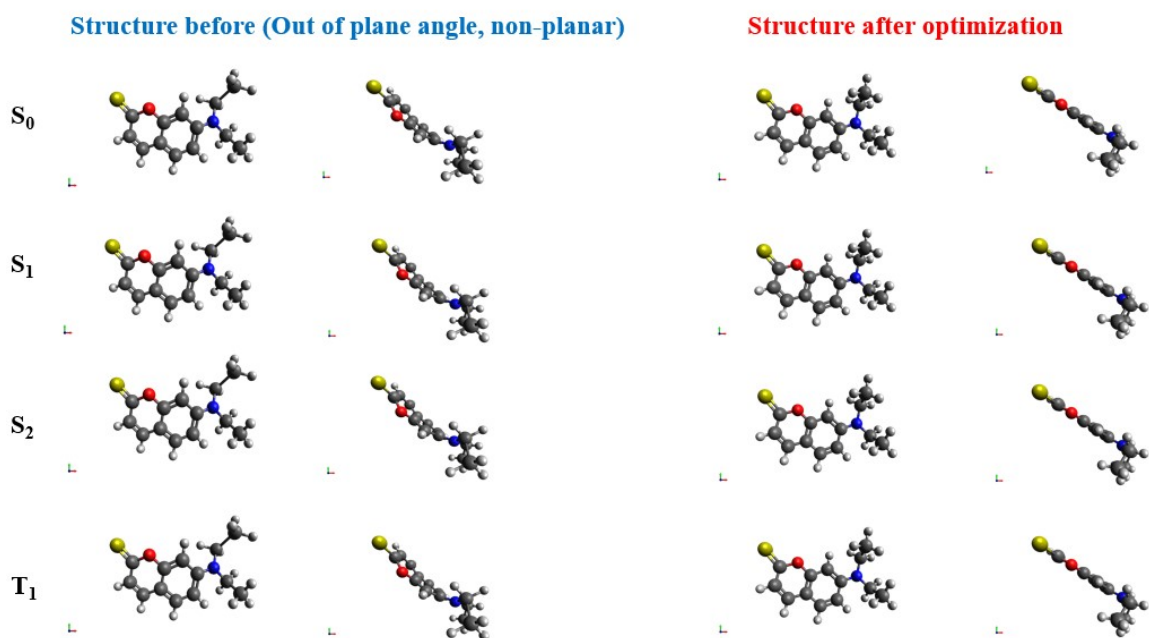


Figure S10. Re-optimized excited geometries of relevant excited states for SCou at the TD-PBE0/CPCM/def2-TZVPD level of theory using the purposely induced non-planar structure as a starting point.

Table S5. Vertical excitation energies (eV) and energy gaps (eV) between relevant singlet and triplet excited states using the S_1 Minimum geometry for SACD computed at the TD-PBE0-D3BJ/CPCM/def2-TZVPD//B3LYP_G-D3BJ/CPCM/def2-TZVPD level of theory. The oscillator strengths are shown in parentheses.

State	ACN	State	DMSO
$S_1(n\pi^*)$	2.180 (0.000)	$S_1(n\pi^*)$	2.182 (0.000)
$S_2(\pi\pi^*)$	3.004 (0.340)	$S_2(\pi\pi^*)$	2.969 (0.363)
$S_3(\pi\pi^*)$	3.584 (0.017)	$S_3(\pi\pi^*)$	3.573 (0.015)
$T_1(\pi\pi^*)$	1.882	$T_1(\pi\pi^*)$	1.884
$T_2(n\pi^*)$	1.965	$T_2(n\pi^*)$	1.970
$T_3(\pi\pi^*)$	2.643	$T_3(\pi\pi^*)$	2.643
$T_4(\pi\pi^*)$	3.332	$T_4(\pi\pi^*)$	3.331
$\Delta E(S_1-T_1)$	0.298	$\Delta E(S_1-T_1)$	0.298
$\Delta E(S_1-T_3)$	-0.463	$\Delta E(S_1-T_3)$	-0.461
$\Delta E(S_1-T_4)$	-1.152	$\Delta E(S_1-T_4)$	-1.149
$\Delta E(S_2-T_2)$	1.039	$\Delta E(S_2-T_2)$	0.999
$\Delta E(S_3-T_2)$	1.619	$\Delta E(S_3-T_2)$	1.603

Table S6. Vertical excitation energies (eV) and energy gaps (eV) between relevant singlet and triplet excited states using the S_2 Minimum geometry for SACD computed at the TD-PBE0-D3BJ/CPCM/def2-TZVPD//B3LYP_G-D3BJ/CPCM/def2-TZVPD level of theory. The oscillator strengths are shown in parentheses.

State	ACN	State	DMSO
$S_1(n\pi^*)$	2.270 (0.000)	$S_1(n\pi^*)$	2.271 (0.000)
$S_2(\pi\pi^*)$	2.986 (0.334)	$S_2(\pi\pi^*)$	2.951 (0.358)
$S_3(\pi\pi^*)$	3.659 (0.044)	$S_3(\pi\pi^*)$	3.645 (0.041)
$T_1(\pi\pi^*)$	1.867	$T_1(\pi\pi^*)$	1.867
$T_2(n\pi^*)$	2.044	$T_2(n\pi^*)$	2.048
$T_3(\pi\pi^*)$	2.673	$T_3(\pi\pi^*)$	2.673
$T_4(\pi\pi^*)$	3.369	$T_4(\pi\pi^*)$	3.368
$\Delta E(S_1-T_1)$	0.403	$\Delta E(S_1-T_1)$	0.404
$\Delta E(S_1-T_3)$	-0.403	$\Delta E(S_1-T_3)$	-0.402
$\Delta E(S_1-T_4)$	-1.099	$\Delta E(S_1-T_4)$	-1.097
$\Delta E(S_2-T_2)$	0.942	$\Delta E(S_2-T_2)$	0.903
$\Delta E(S_3-T_2)$	1.615	$\Delta E(S_3-T_2)$	1.597

Table S7. Vertical excitation energies (eV) and energy gaps (eV) between relevant singlet and triplet excited states using the T_1 Minimum geometry for SACD computed at the TD-PBE0-D3BJ/CPCM/def2-TZVPD//B3LYP_G-D3BJ/CPCM/def2-TZVPD level of theory. The oscillator strengths are shown in parentheses.

State	ACN	State	DMSO
$S_1(n\pi^*)$	2.276 (0.000)	$S_1(n\pi^*)$	2.278 (0.000)
$S_2(\pi\pi^*)$	2.998 (0.338)	$S_2(\pi\pi^*)$	2.963 (0.363)
$S_3(\pi\pi^*)$	3.680 (0.047)	$S_3(\pi\pi^*)$	3.666 (0.044)
$T_1(\pi\pi^*)$	1.863	$T_1(\pi\pi^*)$	1.864
$T_2(n\pi^*)$	2.047	$T_2(n\pi^*)$	2.052
$T_3(\pi\pi^*)$	2.696	$T_3(\pi\pi^*)$	2.696
$T_4(\pi\pi^*)$	3.390	$T_4(\pi\pi^*)$	3.390
$\Delta E(S_1-T_1)$	0.413	$\Delta E(S_1-T_1)$	0.414
$\Delta E(S_1-T_3)$	-0.420	$\Delta E(S_1-T_3)$	-0.418
$\Delta E(S_1-T_4)$	-1.114	$\Delta E(S_1-T_4)$	-1.112
$\Delta E(S_2-T_2)$	0.951	$\Delta E(S_2-T_2)$	0.911
$\Delta E(S_3-T_2)$	1.633	$\Delta E(S_3-T_2)$	1.614

Table S8. Vertical excitation energies (eV) and energy gaps (eV) between relevant singlet and triplet excited states using the S_1 Minimum geometry for SCou computed at the TD-PBE0-D3BJ/CPCM/def2-TZVPD//B3LYP_G-D3BJ/CPCM/def2-TZVPD level of theory. The oscillator strengths are shown in parentheses.

State	ACN	State	DMSO
$S_1(n\pi^*)$	2.956 (0.118)	$S_1(\pi\pi^*)$	2.934 (0.753)
$S_2(\pi\pi^*)$	2.981 (0.669)	$S_2(n\pi^*)$	2.966 (0.069)
$S_3(\pi\pi^*)$	3.868 (0.178)	$S_3(\pi\pi^*)$	3.853 (0.172)
$T_1(\pi\pi^*)$	1.940	$T_1(\pi\pi^*)$	1.940
$T_2(n\pi^*)$	2.729	$T_2(n\pi^*)$	2.735
$T_3(\pi\pi^*)$	2.888	$T_3(\pi\pi^*)$	2.888
$T_4(\pi\pi^*)$	3.574	$T_4(\pi\pi^*)$	3.573
$\Delta E(S_1-T_1)$	1.016	$\Delta E(S_1-T_2)$	0.199
$\Delta E(S_1-T_3)$	0.068	$\Delta E(S_2-T_1)$	1.026
$\Delta E(S_1-T_4)$	-0.618	$\Delta E(S_2-T_3)$	0.078
$\Delta E(S_2-T_2)$	0.252	$\Delta E(S_2-T_4)$	-0.607
$\Delta E(S_3-T_2)$	1.139	$\Delta E(S_3-T_2)$	1.118

Table S9. Vertical excitation energies (eV) and energy gaps (eV) between relevant singlet and triplet excited states using the S₂ Minimum geometry for SCou computed at the TD-PBE0-D3BJ/CPCM/def2-TZVPD//B3LYP_G-D3BJ/CPCM/def2-TZVPD level of theory. The oscillator strengths are shown in parentheses.

State	ACN	State	DMSO
S ₁ (nπ*)	2.758 (0.000)	S ₁ (nπ*)	2.764 (0.000)
S ₂ (ππ*)	2.963 (0.837)	S ₂ (ππ*)	2.921 (0.867)
S ₃ (ππ*)	3.724 (0.094)	S ₃ (ππ*)	3.711 (0.092)
T ₁ (ππ*)	1.910	T ₁ (ππ*)	1.911
T ₂ (nπ*)	2.557	T ₂ (nπ*)	2.565
T ₃ (ππ*)	2.765	T ₃ (ππ*)	2.766
T ₄ (ππ*)	3.492	T ₄ (ππ*)	3.490
ΔE(S ₁ -T ₁)	0.848	ΔE(S ₁ -T ₁)	0.853
ΔE(S ₁ -T ₃)	-0.007	ΔE(S ₁ -T ₃)	-0.002
ΔE(S ₁ -T ₄)	-0.734	ΔE(S ₁ -T ₄)	-0.726
ΔE(S ₂ -T ₂)	0.406	ΔE(S ₂ -T ₂)	0.356
ΔE(S ₃ -T ₂)	1.167	ΔE(S ₃ -T ₂)	1.146

Table S10. Vertical excitation energies (eV) and energy gaps (eV) between relevant singlet and triplet excited states using the T₁ Minimum geometry for SCou computed at the TD-PBE0-D3BJ/CPCM/def2-TZVPD//B3LYP_G-D3BJ/CPCM/def2-TZVPD level of theory. The oscillator strengths are shown in parentheses.

State	ACN	State	DMSO
S ₁ (nπ*)	2.956 (0.000)	S ₁ (ππ*)	2.959 (0.677)
S ₂ (ππ*)	3.004 (0.887)	S ₂ (nπ*)	2.961 (0.243)
S ₃ (ππ*)	3.864 (0.109)	S ₃ (ππ*)	3.852 (0.105)
T ₁ (ππ*)	1.902	T ₁ (ππ*)	1.902
T ₂ (nπ*)	2.736	T ₂ (nπ*)	2.743
T ₃ (ππ*)	2.905	T ₃ (ππ*)	2.906
T ₄ (ππ*)	3.551	T ₄ (ππ*)	3.550
ΔE(S ₁ -T ₁)	1.054	ΔE(S ₁ -T ₂)	0.216
ΔE(S ₁ -T ₃)	0.051	ΔE(S ₂ -T ₁)	1.059
ΔE(S ₁ -T ₄)	-0.595	ΔE(S ₂ -T ₃)	0.055
ΔE(S ₂ -T ₂)	0.268	ΔE(S ₂ -T ₄)	-0.589
ΔE(S ₃ -T ₂)	1.128	ΔE(S ₃ -T ₂)	1.109

Table S11. Functional analysis for calculation of vertical excitation energies for the lowest lying singlet and triplet states in the Franck-Condon region for ACD in ACN with the def2-TZVPD basis set.

State	CAM-B3LYP	State	X3LYP	State	PBE0	PBE0 (TDA OFF)
S ₁ ($\pi\pi^*$)	3.89 (0.196)	S ₁ ($\pi\pi^*$)	3.54 (0.145)	S ₁ ($\pi\pi^*$)	3.62 (0.151)	3.47 (0.117)
S ₂ ($n\pi^*$)	4.18 (0.000)	S ₂ ($n\pi^*$)	3.84 (0.000)	S ₂ ($n\pi^*$)	3.87 (0.000)	3.86 (0.000)
S ₃ ($\pi\pi^*$)	4.62 (0.015)	S ₃ ($\pi\pi^*$)	4.35 (0.014)	S ₃ ($\pi\pi^*$)	4.43 (0.020)	4.37 (0.022)
T ₁ ($\pi\pi^*$)	2.87	T ₁ ($\pi\pi^*$)	2.66	T ₁ ($\pi\pi^*$)	2.68	2.58
T ₂ ($n\pi^*$)	3.71	T ₂ ($n\pi^*$)	3.53	T ₂ ($n\pi/\pi\pi^*$)	3.53	3.29
T ₃ ($\pi\pi^*$)	3.81	T ₃ ($\pi\pi^*$)	3.64	T ₃ ($\pi\pi^*$)	3.62	3.40
T ₄ ($n\pi^*$)	3.83	T ₄ ($\pi\pi^*$)	3.72	T ₄ ($\pi\pi/n\pi^*$)	3.71	3.49

Table S12. Functional analysis for calculation of vertical excitation energies for the lowest lying singlet and triplet states in the Franck-Condon region for ACD in DMSO with the def2-TZVPD basis set.

State	CAM-B3LYP	State	X3LYP	State	PBE0	PBE0 (TDA OFF)
S ₁ ($\pi\pi^*$)	3.87 (0.213)	S ₁ ($\pi\pi^*$)	3.53 (0.157)	S ₁ ($\pi\pi^*$)	3.59 (0.163)	3.46 (0.129)
S ₂ ($n\pi^*$)	4.18 (0.000)	S ₂ ($n\pi^*$)	3.84 (0.000)	S ₂ ($n\pi^*$)	3.87 (0.000)	3.86 (0.000)
S ₃ ($\pi\pi^*$)	4.62 (0.018)	S ₃ ($\pi\pi^*$)	4.35 (0.017)	S ₃ ($\pi\pi^*$)	4.43 (0.023)	4.37 (0.028)
T ₁ ($\pi\pi^*$)	2.87	T ₁ ($\pi\pi^*$)	2.66	T ₁ ($\pi\pi^*$)	2.68	2.58
T ₂ ($n\pi^*$)	3.71	T ₂ ($n\pi^*$)	3.54	T ₂ ($n\pi/\pi\pi^*$)	3.53	3.29
T ₃ ($\pi\pi^*$)	3.81	T ₃ ($\pi\pi^*$)	3.64	T ₃ ($\pi\pi^*$)	3.62	3.40
T ₄ ($n\pi^*$)	3.83	T ₄ ($\pi\pi^*$)	3.72	T ₄ ($\pi\pi/n\pi^*$)	3.71	3.49

Table S13. Functional analysis for calculation of vertical excitation energies for the lowest lying singlet and triplet states in the Franck-Condon region for Cou in ACN with the def2-TZVPD basis set.

State	CAM-B3LYP	State	X3LYP	State	PBE0	PBE0 (TDA OFF)
S ₁ ($\pi\pi^*$)	3.84 (0.854)	S ₁ ($\pi\pi^*$)	3.54 (0.715)	S ₁ ($\pi\pi^*$)	3.61 (0.747)	3.44 (0.604)
S ₂ ($\pi\pi^*$)	4.59 (0.030)	S ₂ ($\pi\pi^*$)	4.29 (0.028)	S ₂ ($\pi\pi^*$)	4.38 (0.027)	4.32 (0.022)
S ₃ ($\pi\pi^*$)	5.20 (0.031)	S ₃ ($\pi\pi^*$)	4.66 (0.085)	S ₃ ($\pi\pi^*$)	4.77 (0.084)	4.64 (0.046)
T ₁ ($\pi\pi^*$)	2.64	T ₁ ($\pi\pi^*$)	2.47	T ₁ ($\pi\pi^*$)	2.49	2.35
T ₂ ($\pi\pi^*$)	3.91	T ₂ ($\pi\pi^*$)	3.72	T ₂ ($\pi\pi^*$)	3.76	3.63
T ₃ ($\pi\pi^*$)	4.00	T ₃ ($\pi\pi^*$)	3.81	T ₃ ($\pi\pi^*$)	3.85	3.75
T ₄ ($\pi\pi^*$)	4.31	T ₄ ($\pi\pi^*$)	4.09	T ₄ ($\pi\pi^*$)	4.12	3.95

Table S14. Functional analysis for calculation of vertical excitation energies for the lowest lying singlet and triplet states in the Franck-Condon region for Cou in DMSO with the def2-TZVPD basis set.

State	CAM-B3LYP	State	X3LYP	State	PBE0	PBE0 (TDA OFF)
S ₁ (ππ*)	3.81 (0.884)	S ₁ (ππ*)	3.50 (0.748)	S ₁ (ππ*)	3.58 (0.781)	3.41 (0.639)
S ₂ (ππ*)	4.58 (0.033)	S ₂ (ππ*)	4.29 (0.030)	S ₂ (ππ*)	4.38 (0.029)	4.31 (0.025)
S ₃ (ππ*)	5.19 (0.032)	S ₃ (ππ*)	4.65 (0.089)	S ₃ (ππ*)	4.76 (0.087)	4.63 (0.049)
T ₁ (ππ*)	2.64	T ₁ (ππ*)	2.47	T ₁ (ππ*)	2.49	2.35
T ₂ (ππ*)	3.91	T ₂ (ππ*)	3.72	T ₂ (ππ*)	3.76	3.63
T ₃ (ππ*)	4.00	T ₃ (ππ*)	3.81	T ₃ (ππ*)	3.85	3.75
T ₄ (ππ*)	4.31	T ₄ (ππ*)	4.09	T ₄ (ππ*)	4.12	3.96

Table S15. Calculated Spin-Orbit Couplings constants for ACD in ACN and DMSO computed at the TD-PBE0-D3BJ/CPCM/def2-TZVPD//B3LYP_G-D3BJ/CPCM/def2-TZVPD level of theory.

FC-Geometry (ACN)		FC Geometry (DMSO)	
S ₂ -T ₁ (¹ nπ* - ³ ππ*)	17 cm ⁻¹	S ₂ -T ₁ (¹ nπ* - ³ ππ*)	17 cm ⁻¹
S ₂ -T ₃ (¹ nπ* - ³ ππ*)	0.76 cm ⁻¹	S ₂ -T ₃ (¹ nπ* - ³ ππ*)	0.77 cm ⁻¹
S ₂ -T ₄ (¹ nπ* - ³ ππ*)	22 cm ⁻¹	S ₂ -T ₄ (¹ nπ* - ³ ππ*)	22 cm ⁻¹
S ₁ -T ₂ (¹ ππ* - ³ nπ*)	13 cm ⁻¹	S ₁ -T ₂ (¹ ππ* - ³ nπ*)	14 cm ⁻¹
S ₃ -T ₂ (¹ ππ* - ³ nπ*)	0.35 cm ⁻¹	S ₃ -T ₂ (¹ ππ* - ³ nπ*)	0.34 cm ⁻¹
S ₁ -T ₁ (¹ ππ* - ³ ππ*)	0 cm ⁻¹	S ₁ -T ₁ (¹ ππ* - ³ ππ*)	0 cm ⁻¹
S ₁ -T ₃ (¹ ππ* - ³ ππ*)	0.01 cm ⁻¹	S ₁ -T ₃ (¹ ππ* - ³ ππ*)	0.01 cm ⁻¹
S ₁ -T ₄ (¹ ππ* - ³ ππ*)	0.01 cm ⁻¹	S ₁ -T ₄ (¹ ππ* - ³ ππ*)	0.01 cm ⁻¹

Table S16. Calculated Spin-Orbit Couplings constants for Cou in ACN and DMSO computed at the TD-PBE0-D3BJ/CPCM/def2-TZVPD//B3LYP_G-D3BJ/CPCM/def2-TZVPD level of theory.

FC-Geometry (ACN)		FC Geometry (DMSO)	
S ₂ -T ₁ (¹ ππ* - ³ ππ*)	0.53 cm ⁻¹	S ₂ -T ₁ (¹ ππ* - ³ ππ*)	0.51 cm ⁻¹
S ₂ -T ₃ (¹ ππ* - ³ ππ*)	0.22 cm ⁻¹	S ₂ -T ₃ (¹ ππ* - ³ ππ*)	0.19 cm ⁻¹
S ₂ -T ₄ (¹ ππ* - ³ ππ*)	0.15 cm ⁻¹	S ₂ -T ₄ (¹ ππ* - ³ ππ*)	0.15 cm ⁻¹
S ₁ -T ₂ (¹ ππ* - ³ ππ*)	0.42 cm ⁻¹	S ₁ -T ₂ (¹ ππ* - ³ ππ*)	0.46 cm ⁻¹
S ₃ -T ₂ (¹ ππ* - ³ ππ*)	0.13 cm ⁻¹	S ₃ -T ₂ (¹ ππ* - ³ ππ*)	0.13 cm ⁻¹

S2.4. Calculated excited state absorption spectra

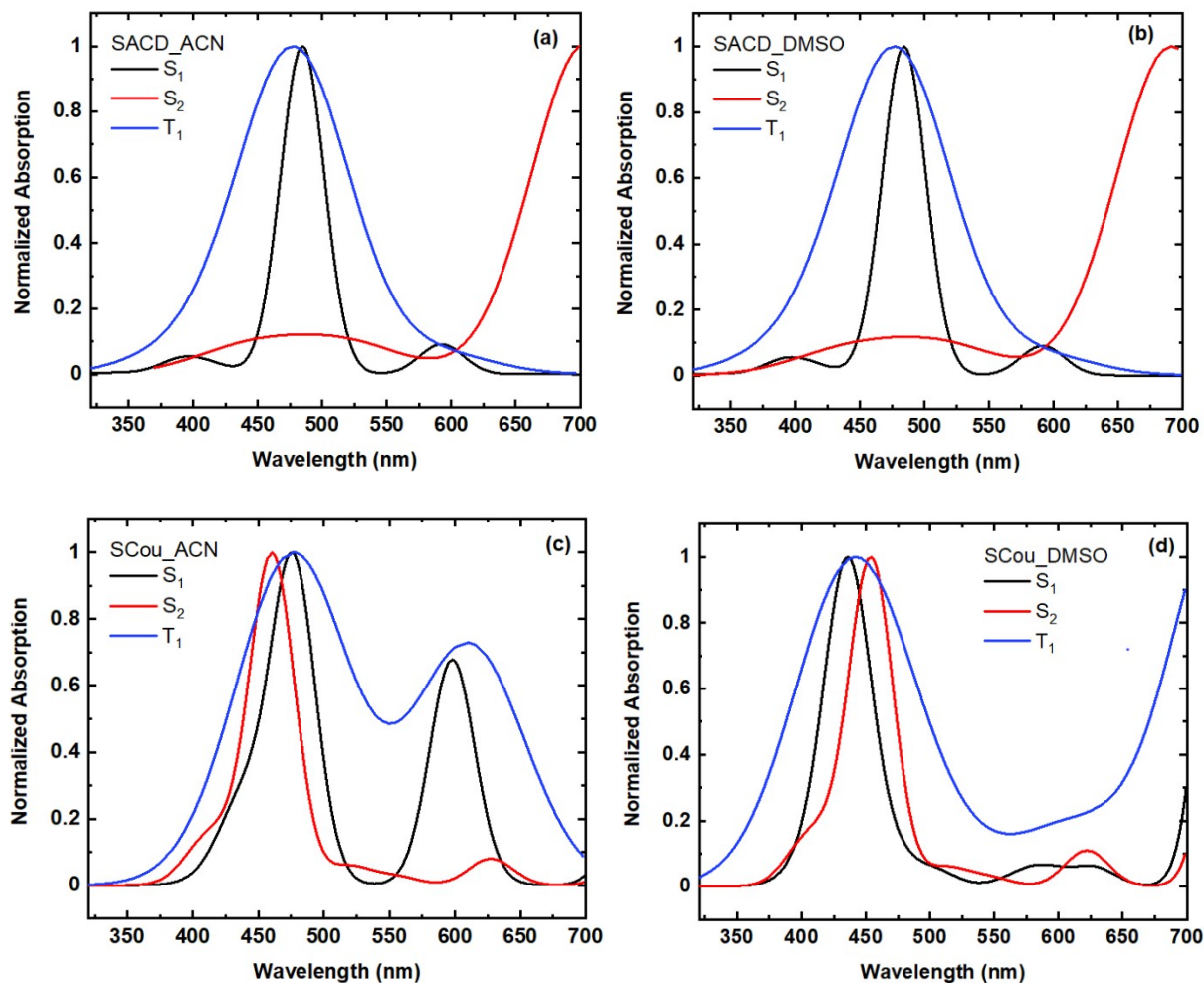


Figure S11. Calculated EAS of S_1 , S_2 , and T_1 states of (a-b) SACD and (c-d) SCou obtained at the TD-PBE0-D3BJ/CPCM/def2-TZVPD level of theory in ACN and DMSO.

The computed EAS spectra for the S_1 , S_2 , and T_1 states of SACD and SCou in both ACN and DMSO are illustrated in Figure S11. These results reveal significant overlap among the three states, aligning with the experimental data shown in Figures 4 and 5 for SACD and Figures 6 and 7 for SCou. The experimental observations highlight a notable overlap of various transient species at initial time delays. Therefore, these EAS spectra have been crucial in elucidating the excited state dynamics of SACD and SCou.

S3. Cartesian coordinates of relevant states

S₀ SACD

C	3.66244121202900	0.19987789333449	-0.00002034819246
C	2.50518120253925	0.93772203817060	0.00054810061840
C	1.23267356114765	0.32363178537238	0.00089139921998
C	1.19740499439484	-1.09199297042649	0.00039832562653
C	2.38632483435620	-1.84561926035396	-0.00015951431910
C	3.60071907861384	-1.20632942204743	-0.00034797502783
C	-0.00000716576212	1.08713628636899	0.00180016829749
C	-1.19731992990812	-1.09204748841088	0.00039961660710
C	-1.23265348509044	0.32357564972279	0.00089290870814
C	-2.50518928378796	0.93760764298005	0.00055135541540
H	-2.54154794287696	2.01694296890931	0.00088842199494
C	-3.66241515073188	0.19970993175881	-0.00001573745105
C	-3.60062846441959	-1.20649439177844	-0.00034376279238
C	-2.38620480085945	-1.84572815948151	-0.00015690611071
H	4.62319173002841	0.69703918805392	-0.00019080959416
H	2.54149076567435	2.01705896447964	0.00088506839219
H	2.32088549954211	-2.92646232623687	-0.00051517052302
H	4.51326329850117	-1.78812797090058	-0.00081700509428
H	-4.62318871548937	0.69682674656816	-0.00018437541637
H	-4.51314607431985	-1.78833467686997	-0.00081185989797
H	-2.32071617290456	-2.92656812065894	-0.00051295091475
N	0.00005730631136	-1.73938515929869	0.00027691693845
H	0.00008038496924	-2.74983201924604	-0.00013687138604
S	-0.00004668195714	2.77753286999070	0.00038100490147

S₀ SCou

C	1.14643468748964	-0.25304949946415	-0.31667972027072
C	0.05472121792170	0.64194870313386	-0.27022154102299
C	-1.22323523079491	0.15457605177286	-0.11550702952134
C	-1.51461566019971	-1.21568282414394	0.01282969074340
C	-0.41910592508935	-2.10134772824794	-0.02089430509192
C	0.86262800638050	-1.64692171328716	-0.17416245599386
H	0.18521643375278	1.70854773466707	-0.35072919849588
C	-2.86396799587763	-1.59094699326139	0.17064622457943
H	-0.60499723499528	-3.16307025856359	0.08247254280960
H	1.66654745759786	-2.36445590715358	-0.18130922721626
C	-3.85321808923668	-0.64591293473385	0.19460841927642
C	-3.54583164309954	0.72787606810342	0.06408367561302
H	-3.11099033440350	-2.64087495672792	0.27243831110735
H	-4.89054692646068	-0.91712325014052	0.31285271607551
O	-2.23725699414100	1.07397995076073	-0.08468232292632
S	-4.65430223822850	1.98057915983828	0.07480072575658
N	2.41686338702257	0.19059796369519	-0.50066668808662
C	3.55350695755450	-0.73069316984820	-0.51860239075754
H	4.35192473614653	-0.23578470325821	-1.06952331676505
H	3.28609440800123	-1.61605974790278	-1.09555590623146
C	2.71134426483850	1.62155136152989	-0.57603620848931
H	1.98026959846552	2.10035980827864	-1.22936126357728
H	3.67698624519842	1.72043421161310	-1.06904548100697
C	4.05531996239515	-1.13196998358599	0.86684644962437
H	4.87533167790267	-1.84607581295751	0.76902679818089
H	4.42214026348651	-0.26462625165559	1.41588063258505
H	3.26417590082562	-1.59938845311846	1.45438473450164

C	2.75084682915047	2.32493013189974	0.77953292767075
H	3.54231320962381	1.91624554142582	1.40760678032118
H	2.94266960934725	3.38983651216129	0.63504257150898
H	1.80459341942554	2.21946098917093	1.31098385509934

S₁ SACD

C	3.66210947124241	0.21297254397759	0.00019285265806
C	2.48847049393401	0.94137088800024	0.00065086731230
C	1.23334709895414	0.30278176435949	0.00054508899828
C	1.20876652707825	-1.11523640650005	0.00007231301245
C	2.39721383485783	-1.83985154792260	-0.00034925674213
C	3.61635360380780	-1.17978795386758	-0.00031129517151
C	-0.00000436613434	1.00427630079932	0.00086722836389
C	-1.20867950971673	-1.11528646534016	0.00019078415722
C	-1.23332627420619	0.30273129749361	0.00041775143771
C	-2.48848175979570	0.94126225047654	0.00026976801594
H	-2.52543933242176	2.02682367445406	0.00037131593164
C	-3.66208047581324	0.21280431375273	-0.00003925874992
C	-3.61625929267408	-1.17995213922276	-0.00005783843144
C	-2.39709329998536	-1.83995872038718	0.00004227993107
H	4.61666336410717	0.72574408655698	0.00024244706624
H	2.52537150886219	2.02693460984037	0.00105230827847
H	2.35202277741035	-2.92375983032499	-0.00072180980832
H	4.53497930470680	-1.75453749474327	-0.00067183577419
H	-4.61666442477415	0.72552655066074	-0.00016994650010
H	-4.53485867631891	-1.75474590344124	-0.00020276401158
H	-2.35185118673984	-2.92386464858195	-0.00005346631031
N	0.00005651807336	-1.75518565046529	0.00006197824635
H	0.00007612761387	-2.76417573864104	-0.00019384534977
S	-0.00004203206788	2.73085421906646	0.00149433343965

S₁ SCou

C	1.15555760643067	-0.26590172905188	-0.31078263241584
C	0.06092927048888	0.62856477066128	-0.21871167866295
C	-1.21422221357174	0.14944124363485	-0.04348584068005
C	-1.49833936472346	-1.22760248166896	0.03379779793694
C	-0.40027572110352	-2.10681757366185	-0.06410226551078
C	0.88546986809430	-1.65701398713821	-0.22129176258771
H	0.19485198974662	1.69934280064509	-0.26482009144277
C	-2.85851433159615	-1.63720806870003	0.14386297865780
H	-0.58981103697020	-3.17339698537482	-0.01618953199702
H	1.68704108203982	-2.37756650667880	-0.28788311953043
C	-3.82890668435982	-0.65113498188158	0.18344215578871
C	-3.51911029032138	0.71044757659241	0.13801966789536
H	-3.11347373550354	-2.68776403792616	0.18089714998997
H	-4.87776094458848	-0.90924736465587	0.25080023905225
O	-2.19495958300522	1.09042682188115	0.04490019033515
S	-4.62870280650733	1.98243286914741	0.19037256961105
N	2.41542326822593	0.20078980788951	-0.48815860021608
C	3.55665535375883	-0.69708436044062	-0.45974396412637
H	4.38859886928787	-0.16721174138920	-0.92213396600809
H	3.34280776710131	-1.56402812522273	-1.09017448083147
C	2.68492627105368	1.61974138643121	-0.63554333931670
H	1.89774046056299	2.06783623768773	-1.24406014498845
H	3.61200593950793	1.70888254413477	-1.20275286467326
C	3.94476776721712	-1.14673171809857	0.94299211826887
H	4.78668301467146	-1.83866823097463	0.87527712742795
H	4.24464227500503	-0.29659583919386	1.55669284681497
H	3.11802471534904	-1.65810433987211	1.43860696700079
C	2.81852021216450	2.35789477474238	0.69039298759277
H	3.66038703834591	1.97579442338788	1.26893916546525
H	2.98935913323540	3.41810764573002	0.49241547607544

H 1.91154480996351 2.25931516936422 1.28948484507468

S₂ SACD

C 3.66450358193950 0.18128635461707 0.00029658622530

C 2.49870035977366 0.94085761048243 0.00026812655957

C 1.23600908739375 0.33685289930392 0.00015418704686

C 1.20646453451849 -1.08797002940625 -0.00004815971291

C 2.37759408230056 -1.84785758153451 0.00001440855891

C 3.60804943049528 -1.20878239630761 0.00021583901059

C -0.00001115803377 1.06966020000063 0.00031784144365

C -1.20637825506421 -1.08802713476262 -0.00023313612241

C -1.23599874555589 0.33679433284154 0.00032877084362

C -2.49871660901150 0.94075296592998 0.00080341976254

H -2.54596028258997 2.02188680073863 0.00132681658131

C -3.66447669255298 0.18112419949448 0.00063510143037

C -3.60794288433354 -1.20893826769691 -0.00013543938387

C -2.37747089905855 -1.84797049158495 -0.00053716398465

H 4.62561676525733 0.68210850005435 0.00042249442567

H 2.54590399483223 2.02199445101556 0.00039285567159

H 2.30449683960907 -2.92987447507283 -0.00009871573482

H 4.51956236883585 -1.79399295417937 0.00029061300593

H -4.62561819641502 0.68188855098553 0.00102228554103

H -4.51943117174733 -1.79419254019876 -0.00035422638926

H -2.30433508657610 -2.92998377593076 -0.00101032475305

N 0.00005820414290 -1.70944995504998 -0.00034910064024

H 0.00008348442111 -2.72309214491578 -0.00055539042808

S -0.00005275258084 2.78266488117624 0.00053231104230

S₂ SCou

C	1.15663249062196	-0.25503828714434	-0.34839345688864
C	0.05612512575779	0.62683013762558	-0.35667481097382
C	-1.21781514755031	0.14832344340574	-0.16727205515865
C	-1.51413563404237	-1.21038785639199	0.04100367212193
C	-0.40899209050398	-2.07434361834895	0.04480370536234
C	0.88016013733001	-1.62397923995721	-0.13444745288824
H	0.18016235313041	1.69105766179873	-0.49847692259407
C	-2.86383652834313	-1.60099672979701	0.23881048411668
H	-0.58283594215460	-3.13331476873760	0.20469264505876
H	1.68610444310441	-2.34295902361057	-0.09978846069885
C	-3.84905668567810	-0.61777392299782	0.21657839563527
C	-3.50859968153781	0.68821331229268	0.00107107319278
H	-3.11564550518304	-2.64072697150559	0.39934429349000
H	-4.89505860045962	-0.86044862352216	0.35854166143727
O	-2.22127661964990	1.09062765178666	-0.18789598396527
S	-4.60423573021875	2.03123280426601	-0.04041699629647
N	2.42879310005047	0.20114784883755	-0.54438413930941
C	3.55139814240594	-0.71503557269618	-0.57032686155454
H	4.34692695799829	-0.22951210939671	-1.13967722222119
H	3.26730972305865	-1.60317363659680	-1.14076808580260
C	2.71566265085292	1.62246878724846	-0.53207565414089
H	2.02267162546961	2.13979431615903	-1.20254340486475
H	3.70855497108409	1.75065007047927	-0.96592409582878
C	4.08107811702394	-1.12137363282811	0.79741024362561
H	4.89380533828809	-1.84271729824036	0.68091730147807
H	4.46889309522803	-0.25813463548302	1.34120040779480
H	3.30024947178936	-1.58413937356805	1.40454699834925
C	2.67434146599489	2.25811706540285	0.85060666176758
H	3.43194547861182	1.82187817983058	1.50386303858500
H	2.86383278965821	3.33159349258495	0.77565294712117

H	1.69870068786269	2.11906052910438	1.32108207404962
---	------------------	------------------	------------------

T₁ SACD

C	3.66550820533071	0.17557892260380	0.00036258658410
C	2.50786163475653	0.93827326083417	0.00052237540606
C	1.23933748696483	0.34506026646191	0.00031807779673
C	1.21047436046862	-1.07794764109296	-0.00007626662074
C	2.37719104024112	-1.84310437726090	-0.00023161173921
C	3.60892455099770	-1.21685467757017	-0.00000992949766
C	-0.00000973780658	1.07605479022194	0.00046180507366
C	-1.21038926565248	-1.07799976194100	-0.00007242103429
C	-1.23932477553216	0.34500712786194	0.00031395746993
C	-2.50787722732685	0.93816741697402	0.00050946647716
H	-2.56563918585942	2.01866922739173	0.00077438417065
C	-3.66548011622410	0.17541554790262	0.00036916891761
C	-3.60882357034252	-1.21701403793665	-0.00000140188204
C	-2.37706825263942	-1.84321171916928	-0.00023275707672
H	4.62813623098841	0.67427107952030	0.00053010831724
H	2.56557569588761	2.01877753391749	0.00080226308060
H	2.29614541008348	-2.92480387031691	-0.00050842697321
H	4.51770573261907	-1.80527951666178	-0.00012355327176
H	-4.62813402300125	0.67405087628887	0.00053884775220
H	-4.51757536631143	-1.80548424162674	-0.00009488576220
H	-2.29597580397688	-2.92490739068738	-0.00050690643254
N	0.00005688803662	-1.70530958880197	-0.00026805706610
H	0.00007868462084	-2.71818148380882	-0.00050354480020
S	-0.00004859632250	2.78851225689579	0.00082672111067

T₁ SCou

C	1.15785568047922	-0.26691673387645	-0.32392116037560
C	0.05959312512594	0.63319495133853	-0.27330342513423
C	-1.21213017894905	0.16834256207090	-0.10302962623137
C	-1.50845032638205	-1.21809756766231	0.02001811278202
C	-0.40593993421255	-2.09906621950161	-0.02807757720941
C	0.87887075493432	-1.65183393157938	-0.18978093531653
H	0.19857356091652	1.70097385483715	-0.35911689148450
C	-2.84769998436674	-1.61703943570106	0.17106855296970
H	-0.59410547579828	-3.16214637786770	0.06885064761679
H	1.68091921161758	-2.37521948228372	-0.20840277108474
C	-3.82908334934894	-0.61904414761979	0.20031670136463
C	-3.52572793601068	0.72696037146449	0.09134359111157
H	-3.10661115440510	-2.66265233048027	0.25494906831142
H	-4.87439344035286	-0.87706748509406	0.31069645996087
O	-2.19937688683868	1.10668650903536	-0.05717609918056
S	-4.63710122702060	1.99077407467785	0.11622331631698
N	2.42041631399633	0.18630048297964	-0.49859718039295
C	3.55501473035297	-0.72495071407949	-0.51009048097605
H	4.35851515618793	-0.22172515732672	-1.04806468072071
H	3.29375936076310	-1.60835739903213	-1.09521473340491
C	2.70360564977680	1.61113246759413	-0.58417379145184
H	1.97123913630957	2.07638896053994	-1.24730006080821
H	3.67377925642415	1.71211897817938	-1.07030337451326
C	4.03033749714459	-1.12621243757903	0.87794245725677
H	4.86228240507975	-1.82770320623146	0.78687844665141
H	4.37507186785290	-0.25854925245176	1.44219080374729
H	3.23294329530302	-1.61145767814279	1.44407546005582
C	2.72425711912885	2.31584628388598	0.76399422570474
H	3.51309053622815	1.91804083412807	1.40368639129557
H	2.91101539017732	3.38075910312159	0.61037722902592

S4. Supporting references.

1. J. Tang, L. Wang, A. Loredó, C. Cole and H. Xiao, *Chem. Sci.*, 2020, **11**, 6701–6708.
2. F. Neese, Wiley Interdisciplinary Reviews: *Comput. Mol. Sci.*, 2012, **2**, 73-78.
3. S. Mai, M. Pollum, L. Martínez-Fernández, N. Dunn, P. Marquetand, I. Corral, C. E. Crespo-Hernández and L. Gonzalez, *Nat. Commun.*, 2016, **7**, 1–8.
4. F. Weigend, & R. Ahlrichs, *Phys. Chem. Chem. Phys.*, 2005, **7**, 3297-3305.
5. V. Barone, & M. Cossi, *J. Phys. Chem. A*, 1998, **102**, 1995-2001.
6. C. Reichardt, & C. E. Crespo-Hernández. *J. Phys. Chem. Lett.*, 2010, **1**, 2239-2243.
7. C. Reichardt and C. E. Crespo-Hernández, *Chem. Commun.*, 2010, **46**, 5963–5965
8. J.J. Snellenburg, S. Liptonok, R. Seger, K. M. Mullen, I. H. M. Van Stokkum, *J. Stat. Softw.*, 2012, **49**, 1–22.
9. Y. Yagci, S. Jockusch, N. J. Turro, *Macromolecules*, 2007, **40**, 4481–4485.
10. R. Schmidt, C. Tanielian, R. Dunsbach and C. Wolff, *J. Photochem. Photobiol. A Chem.*, 1994, **79**, 11–17.